

# A Mini Review on the Effects of Synthesis Conditions of Bimetallic Ag/Si Nanoparticles on Their Physicochemical Properties

Nur Syazwanie Abdul Aziz<sup>1</sup>, Norain Isa<sup>1,2,\*</sup>, Mohamed Syazwan Osman<sup>1,3</sup>,  
Wan Zuraida Wan Kamis<sup>1</sup>, Mohamad Sufian So'aib<sup>1</sup> and  
Mohd Azahar Mohd Ariff<sup>1</sup>

<sup>1</sup>Centre for Chemical Engineering Studies, Universiti Teknologi MARA, Cawangan Pulau Pinang, 13500 Permatang Pauh, Pulau Pinang, Malaysia

<sup>2</sup>Waste Management and Resource Recovery (WeResCue) Group, Centre for Chemical Engineering Studies, Universiti Teknologi MARA, Cawangan Pulau Pinang, 13500 Permatang Pauh, Pulau Pinang, Malaysia

<sup>3</sup>EMZI-UiTM Nanoparticles Colloids & Interface Industrial Research Laboratory (NANO-CORE), Centre for Chemical Engineering Studies, Universiti Teknologi MARA, Cawangan Pulau Pinang, 13500 Permatang Pauh, Pulau Pinang, Malaysia

(\*) Corresponding author: norain012@uitm.edu.my  
(Received: 06 July 2022 and Accepted: 01 September 2022)

## Abstract

*In recent decades, nanotechnology-based treatments have made significant strides. Compared to monometallic nanoparticles, bimetallic nanoparticles have gained a great deal of technological and scientific interest due to their superior properties in various applications, which include the treatment of infectious disorders. Bimetallic nanoparticles are created by combining two distinct metals. Among the several bimetallic nanoparticles, silver-silica (Ag/Si) composites hold the most promise for fixing this problem. Ag/Si composites can be manufactured in many shapes, sizes, and structures by supporting them on their organic or inorganic counterparts. The characteristics of Ag/Si composites are superior to those of bimetallic nanoparticles. There are numerous obstacles involved with the characterization of composite materials. Due to the nanomaterials' strong reactivity and high accessible surface area, they are typically unstable and susceptible to coarse agglomeration. It is advised that the surface of nanoparticles be modified to prevent aggregation and agglomeration. Nanomaterials' behavior may impact the physicochemical properties of aggregates. This study examines the parameters that influence the synthesis of Ag/Si under varying conditions, including the effect of initial concentration of metal precursor, reaction time, reaction temperature, and calcination temperature. Based on several prior studies, the properties of the produced Ag/Si composites were subsequently reviewed via transmission electron microscopy (TEM), X-ray diffraction (XRD), X-ray photoelectron microscopy (XPS), energy dispersive X-ray (EDX), and Fourier transform infra-red (FTIR). The highlighted physicochemical properties are shape, crystallinity, and compositions. As a result of their decreased size and increased surface area, Ag/Si composites are widely utilized as catalysts. Drug delivery, water filtration, and catalysis are some of the applications of silver-silica nanocomposites.*

**Keywords:** Silver-silica composite, Synthesis condition, Physicochemical, Bimetallic, Characterization.

## 1. INTRODUCTION

Technology has indeed become the major driving factor for the growth of the economy. By definition, nanotechnology entails the science and engineering involved in the design, synthesis, characterization, and application of materials in dimensions

between 1 and 100 nm [1]. Nanotechnology is helping diverse industrial sectors such as pharmaceutical, food safety, and environmental science by improvising and revolutionizing the technological advances in devices to the microscopic level [2 - 5].

Nanomaterial is becoming one of the propitious topics in many different fields. In fact, the properties of nanoparticles are influenced by the physical and chemical characteristics of the nanomaterials.

The physicochemical properties of nanoparticles encompass the size, surface area, solubility, chemical composition, shape, crystal structure, surface morphology, and stability [6 - 10]. The shape of nanoparticles varies into, planar, tubular, elongated, or the most commonly spherical. The size and shape of nanoparticles impose a significant influence on their performance. Hence, morphological study is important to evaluate the size, shape, and surface of nanoparticles. Moreover, the stability of a dispersed suspension could be determined from the surface charge of nanoparticles. The structure of nanoparticles may present as regular crystalline, amorphous, or forming a pseudo-close packing indistinguishable by any crystallographic space group. For nanomaterials applications, investigation on the crystallinity structure of nanoparticles is crucial.

As a result, bimetallic nanoparticles have recently received more attention than monometallic nanoparticles [11 - 17]. The specific metals that make up bimetallic nanoparticles and contribute to the nanometric size, determine the overall characteristics of the nanoparticles. In the development of bimetallic nanoparticles, several structural components are fused with nanoparticles. For instance, plasmon absorption bands can be improved by altering the tilt of metallic mixtures [18] to manufacture a variety of biosensors. In contrast to pure elemental particles, nanoparticles may yield a range of consequences due to their distinct qualities i.e., size, and electrical, thermal, and catalytic capabilities [19].

Over the past decade, extensive research works on bimetallic nanoparticles were initiated and progressively expanded. In terms of the preparation and precise

characterization of nanoparticles, numerous approaches have been suggested. Recently, researches are directed more toward the selective preparation of novel bimetallic nanoparticles in various forms, including alloys [20], core-shell [21], and contact aggregate [22]. Through bi-metallization, the catalytic characteristics of the resultant nanoparticles could be significantly enhanced, which is not necessarily possible with monometallic catalysts. In catalysis, the electronic effect presented by bimetallic nanoparticles which characterizes charge transfer plays an essential role. Moreover, the structure of bimetallic nanoparticles could be altered by alloying the constituent elements. An additional degree of freedom is introduced in bimetallic nanoparticles, followed by a comparative study on the catalytic activity of various bimetallic nanoparticles. With the aid of physical and spectroscopic data, numerous synthesis approaches and correlations have been established. Indeed, the structure and miscibility of bimetallic nanoparticles are determined from the conditions of preparation. Bimetallic nanoparticles are generally synthesized through simultaneous reduction of two metal ions in an appropriate stabilization method such as steric hindrance and static-electronic repulsive force [23]. Using this method, a particle structure of core-shell to homogeneous alloy is obtainable, depending on the reduction conditions. Moreover, by controlling the size, shape, and structure of the nanoparticles, the reduction rates of the two components could be manipulated.

Numerous scientists have invented various nanoparticle synthesis techniques which are commonly classified into physical, chemical, or biological methods. These include chemical vapor deposition [24], vapor-phase synthesis [25], reduction [26, 27], hydrothermal synthesis [28], sonochemical approach [29], and the standard sol-gel method [30]. Due to their distinctive physical and chemical properties, silver and its compounds are

one of the most widely employed metallic particles in a variety of industries. The diverse potential applications of these materials have urged researches on the synthesis of silver, particularly with silica. Indeed, synthesis parameters could greatly influence the structure, particle size, stability, porosity, and surface properties of the synthesized material. Among the characteristics of a composite material that could be investigated are the sheet thickness, morphological characteristics, lateral dimensions, and compositions variation.

Apart from synthesis, characterization plays an important role in the investigation of the nanomaterials' properties. To date, many techniques are available to characterize nanoparticles, including ultraviolet-visible (UV-Vis) spectroscopy, zeta potential (ZP) analysis, transmission electron microscopy (TEM), Fourier transform infrared (FTIR) spectroscopy, X-ray diffraction (XRD), scanning electron microscopy (SEM), atomic force microscopy (AFM), thermogravimetric analysis (TGA), and energy dispersive X-ray (EDX) spectroscopy. TEM and SEM are commonly employed in the characterization of the size, surface area, and morphology of nanoparticles. Meanwhile, ZP and XRD analyses are practiced to determine the charge stability and the crystallinity structure of nanoparticles, respectively.

Due to the wide application of silver nanoparticles (AgNPs) and their composites in various industries, the properties such as size, shape, and composition have become more challenging to control. As an alternative, surface modification of nanoparticles is recommended to avoid aggregation which may further degrade the mechanical properties of the nanomaterials [31, 32]. One of the major disadvantages of extremely small nanoparticles is the difficulty to maintain good particles dispersion. Aggregation could affect physicochemical properties through the

behavior of a nanomaterial. Since AgNPs are reactive, strategies for synthesizing and effectively stabilizing them with modification to narrow size distribution must be developed to prevent aggregation in solutions.

A composite of Ag and Si exhibits enhanced properties for antimicrobial, biomedical, wastewater remediation, and galvanic displacement applications. The synthesis of Ag/Si composite could be advantageous towards the dispersion of discrete silver particles throughout silica, which consequently prevents agglomeration. The unique structure of silica could act as a suitable carrier for incorporating silver nanoparticles into some materials for industrial use. The properties of a nanomaterial may differ from its bulk materials even with similar chemical composition.

Challenges in characterization may surface from the different materials and chemicals used. Therefore, in this current study, various synthesis conditions such as concentration, time of reaction, and calcination temperature were evaluated to determine the physicochemical properties of Ag/Si composite, including its size, shape, and surface state.

## 2. METHODOLOGY

This paper focuses on the synthesis method and the effect of varying experimental parameters, including the concentration of metal precursor, retention time, reaction temperature, and calcination temperature, in the preparation of Ag/Si nanocomposite. The characteristics of Ag/Si composite were examined through a series of analysis and characterization approaches. The physicochemical parameters of Ag/Si composite were investigated from relevant research publications related to the morphology, crystallinity structure, and chemical compositions of the composite.

The main issue identified from the literature study is the parameters required to synthesize Ag/Si composite to avoid

aggregation. In the first stage of the study, relevant articles and journals were extracted from databases containing pertinent keywords. For this investigation, the keywords included silver nanoparticle, silica nanoparticle, composite, and synthesis method. ScienceDirect, Springer, and ResearchGate were among the databases utilized for the mini reviewing process. The related journals bearing the pertinent keywords were then analyzed, categorized, and recorded in Microsoft Excel.

Several features, including the year of publication, journal title, objectives, methods, parameters, and applications, have been extracted from the collected publications. Master Table was created to compute the proportion of studies based on particular parameters and technique analysis. In accordance with the specified criteria, the synthesized composites were also characterized and their properties were discussed in details. Summary of the research methodology is depicted in Figure 1.

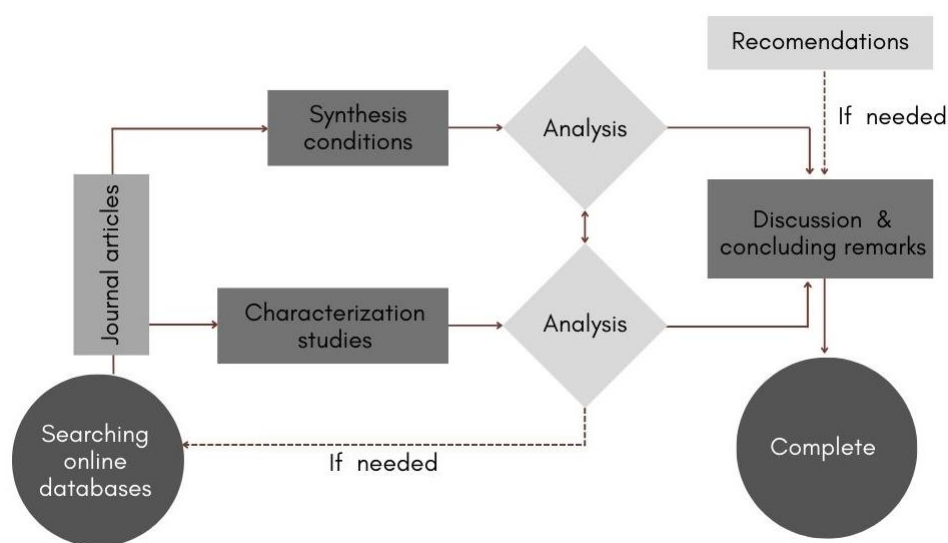


**Figure 1.** Research methodology.

### 3. RESULTS AND DISCUSSION

#### 3.1. Process Conditions

Process conditions play a crucial role in determining the characteristics of silver/silica (Ag/Si) composite throughout its manufacturing process. This section discusses the various procedures to synthesize Ag/Si composite, as well as the different methods of characterization to determine its physicochemical properties. Parameters such as initial metal precursor concentration, reaction temperature, pH, and calcination temperature at formation have, individually or in combination, impose effects toward the properties of the synthesized Ag/Si composite. The various types of procedure are elaborated in following sub-section.

#### 3.2. Effect of Initial Concentration of Metal Precursor

The intrinsic reactivity of a metal precursor presents a major influence on the shape and size of nanoparticles. Precursor concentration could control the number of nuclei formed during the nucleation stage. According to Table 1, a number of previous investigations utilizing various concentrations of silver and silica metal precursor have been undertaken. Majority of the investigations utilized varied concentration ranges of AgNO<sub>3</sub> as the metal precursor for the formation of silver nanoparticles (AgNPs). Based on the studies, a lower initial concentration of a metal precursor contributes to a lower concentration of the active dispersant.

**Table 1.** Summary of Ag/Si synthesis using different concentrations of metal precursors.

| Metal Precursor (AgNPs, SiNPs) |                       | Concentration of Metal Precursor       | Size (nm)   | Shape                   | Crystallinity (Lattice Structure)  | Composition               | Ref. |
|--------------------------------|-----------------------|--|---|-------------------------|--|---------------------------|------|
| Silver nitrate                 | Sodium trisilicate    | 0.034%<br>0.151%<br>0.369%             | 10 – 20<br>(Size increased as concentration increased)          | Honey comb<br>Spherical | FCC<br>(100) – 37.09°  | nd                        | [33] |
| Silver perchlorate             | TEOS                  | 1 -15 mM                               | 28 to 76<br>(Size increased as concentration of TEOS increased) | Spherical               | nd   | Ag<br>Si<br>O             | [34] |
| Silver nitrate                 | TEOS                  | 0.05<br>0.2<br>0.3<br>0.4<br>0.5       | 11<br>24<br>37<br>63<br>90                                      | Irregular               | FCC<br>(111) – 38.1°<br>(200) – 44.3°<br>(220) – 64.5°                                   | nd                        | [35] |
| Silver nitrate                 | Silica from rice husk | 0.3<br>0.4<br>0.5<br>0.6<br>0.7<br>0.8 | 6 – 422<br>(Size increased as concentration increased)          | Ellipsoidal             | FCC<br>(111) – 38.9°<br>(200) – 48.5°<br>(220) – 63.0°<br>(311) – 77.5°<br>(222) – 82.6° | O<br>Si<br>Ag<br>Na<br>Cl | [36] |
| Silver nitrate                 | TEOS                  | 1 mmol<br>2 mmol<br>3 mmol<br>4 mmol   | ±20   | Spherical               | FCC<br>(111) – 38.4°<br>(200) – 44.6°<br>(220) – 64.7°<br>(311) – 77.6°                  | Si<br>Ag<br>O             | [37] |
| Silver nitrate                 | Sodium trisulfate     | 1 mM<br>2 mM<br>3 mM                   | ±17.05  | Quasi-spherical         | FCC<br>(111) – 37.7°<br>(200) – 44.0°<br>(220) – 64.3°<br>(311) – 77.1                   | Si<br>Ag<br>C<br>N<br>O   | [38] |
| Biamminesilver nitrate         |                       | 0.02 M<br>0.08M<br>0.15 M              | 7 – 11<br>(Size increased as concentration increased)           | Spherical tubular       | FCC<br>(111) – 38.1°<br>(200) – 44.3°<br>(220) – 64.5°<br>(311) – 77.5                   | Ag<br>Si                  | [39] |
| Silver nitrate                 | Tetraethoxy-silane    | 6%<br>12%<br>20%<br>50%                | 6<br>8<br>20  | Spherical               | FCC<br>(111) – 34°<br>(200) – 44°<br>(220) – 64°   | nd                        | [40] |
| Silver perchlorate             | TEOS                  | 1 -15 mM                               | 28 to 76<br>(Size increased as concentration increased)         | Spherical               | nd   | Ag<br>Si<br>O             | [34] |

nd: not discussed

TEOS: tetraethyl orthosilicate

Consequently, as the concentration of the reactant decreases, smaller nuclei will develop. In other words, a higher concentration of metal precursors results in larger particle sizes. Moreover, at a higher concentration of precursor, the agglomeration of particles may be associated with the higher surface energy

[41]. Furthermore, the presence of a large amount of precursor creates high attraction between atoms [42], where the atoms tend to attract to one another to promote agglomeration and aggregation of nanoparticles [27, 43]. However, other researchers have noticed that a large number of nuclei are present in Ag/Si

composites prior to the development phase, which promotes particle aggregation when a high concentration of metal precursor is present [44,45]. Furthermore, the development of homogeneous nuclei also facilitates the production of uniformly distributed nanoparticles [46].

### 3.3. Effect of Retention Time and Temperature

The particle size of nanoparticles can be affected by the effect of retention time and temperature. Indeed, the synthesis of nanoparticles is proportional to the rate of reaction, while the stability of nanoparticles is proportional to the duration of reaction [47,48]. The particle size of nanoparticles may increase with increasing reaction time, through deposition and dissolution

processes. Table 2 summarizes the synthesis of Ag/Si composite at different retention time. Based on observation of the obtained results from various studies, it was proven that a higher retention time could lead to the formation of particles of larger diameter. At a lower retention time, agglomeration of AgNPs in the composite is possible, which could produce smaller particles than at a higher retention time. Therefore, the higher is the retention time, more AgNPs are immobilized onto the surface of silica nanoparticles (SiNPs). From the studies, spherical, quasi-spherical, and irregular shaped SiNPs were observed. The adhesion between AgNPs and SiNPs is viable due to the shape change of the nanoparticles [49].

**Table 2.** Effect of retention time on the size, shape, and dispersion of particles.

| Composite | Time of Reaction (hr)           | Size (nm)  | Shape           | Dispersion   | Ref. |
|-----------|---------------------------------|--|-----------------|--|------|
| Ag/Si     | 3.0<br>2.0                      | 34.20<br>16.60   | Spherical       | Un-agglomerated  | [50] |
| Ag/Si     | 1.0<br>3.0<br>5.0<br>7.0<br>9.0 | 13.30 – 25.20<br>(Size increased with increasing reaction time)    | Spherical       | Agglomerated<br>Un-agglomerated<br>Un-agglomerated<br>Un-agglomerated<br>Un-agglomerated | [51] |
| Ag/Si     | 0.2<br>2.0                      | 6.90<br>10.60  | Quasi-spherical | Agglomerated<br>Un-agglomerated  | [52] |
| Ag/Si     | 1.0<br>2.0<br>3.0               | 20.00 – 40.00<br>(Size increased with increasing reaction time)    | Irregular       | Agglomerated   | [53] |
| Ag/Si     | 0.5<br>3.0                      | (Size increased with increasing reaction time based on SEM images) | Irregular       | Agglomerated   | [49] |

Table 3 provides a summary of prior researches on the effect of temperature on the physicochemical properties of nanoparticles. It can be concluded that high temperatures favor nucleation while low temperatures promote growth in the field of wet chemical nanoparticle manufacturing, as is often known [54]. This is because the particle size would decrease as the temperature of the reaction increases. In other words, larger nanoparticles are

formed at lower temperatures. However, it has been shown that the total reaction rate increases as the reactive temperature rises [27]. In conclusion, elevated temperatures may enhance nucleation. On the basis of the aforementioned conclusions, it is possible to deduce that when the reaction temperature increases, the nucleation rate constant will increase while the growth rate constant will decrease.

**Table 3.** Effect of reaction temperature on the properties of various Ag/Si composites.

| Composite                    | Temperature (°C)       | Time of Reaction | Size (nm)            | Shape                      | Crystallinity (Lattice Structure)   | Composition                     | Ref. |
|------------------------------|------------------------|------------------|----------------------|----------------------------|---|---------------------------------|------|
| Ag/Si                        | 100<br>200             | 2                | 360 x 60<br>70 - 100 | Needle-shaped<br>Spherical | nd  | O, Na, Mg, Si,<br>Ag, Cl, K, Ca | [55] |
| Ag/SiO <sub>2</sub> /A<br>PS | Ambient<br>temperature | >24              | 20                   | Spherical                  | FCC<br>(111) – 37.8°<br>(200) – 44.3°<br>(220) – 64.2°<br>(311) – 77.42°    | nd                              | [56] |
|                              | 80                     | 5                | 100                  |                            |   |                                 |      |
| Ag/Si                        | 400                    | 60 min           | 10                   | Spherical                  | FCC<br>(111) – 37.8°<br>(200) – 44.3°<br>(220) – 64.2°<br>(311) – 77.42°    | Si, O, C, Ag                    | [57] |
|                              |                        | 150 min          | 13                   |                            |   |                                 |      |
|                              | 600                    | 60 min           | 16                   |                            |   |                                 |      |
|                              |                        | 150 min          | 20                   |                            |   |                                 |      |
| Ag/Si                        | 400                    | 60 min           | 12                   | Spherical                  | FCC<br>(111) – 38.2°<br>(200) – 44.5°<br>(220) – 64.6°<br>(311) – 77.4°     | Si, O, C, Ag                    | [57] |
|                              |                        | 150 min          | 16                   |                            |   |                                 |      |
|                              | 600                    | 60 min           | 18.5                 |                            |   |                                 |      |
|                              |                        | 150 min          | 21                   |                            |   |                                 |      |
| Ag/Si                        | 150<br>300             | 30 min<br>3 hr   | ±20                  | Octahedron                 | nd  | nd                              | [49] |
| Ag/Si                        | 40                     | 10 min<br>2 hr   | 10.6                 | Quasi-<br>spherical        | FCC<br>(111) – 38.51°<br>(200) – 44.30°<br>(220) – 64.35°<br>(311) – 77.35° | Si, Ag, C, N,<br>O              | [52] |
| Ag/Si                        | 27                     | 16 hr            | 13.03 ±<br>0.19      | Spherical                  | FCC<br>(111) – 38.4°<br>(200) – 44.6°<br>(220) – 78.0°<br>(311) – 82.2°     | C, O, Na, Si                    | [58] |

nd: not discussed

The influence of temperature and time on the size of silver nanoparticles is accountable from the thermal sintering process. Silver ions are contained in the silica fibres cluster to produce nanoparticles by forming a cluster of ions. With a rise in temperature, nanoparticles agglomerate, resulting in a growth in the size of the silver nanoparticles. Due to the interference of the hard silica walls of the porous fibres which prohibit the fusion of individual nanoparticle with the neighboring particles, the size of these nanoparticles reaches a maximum as temperature increases.

Based on previous studies as stated in Table 3, the data of diffraction of peaks at  $2\theta$  confirmed a crystalline presence as corresponded to the JCPDS standard. In specific, the peaks corresponded to the indexed plane reflection of face-centered cubic metal silver. At higher retention time and temperature, higher crystallinity compounds were observed from the narrower peaks. On the other hand, the undetectable peaks indicated the presence of amorphous SiO<sub>2</sub>. To support the XRD results, the analyses of EDS and EDX also revealed the presence of silver, silicon, and oxygen atoms.

### 3.4. Effect of Calcination Temperature

Table 4 demonstrates a few studies on composite synthesis utilizing further thermal treatment by varying calcination temperature. From observation, a higher calcination temperature yielded particle of larger mean diameter and mostly in

spherical shape. In the heat treatment, the number of deprotonated molecules increases as temperature increases. A rapid hydrolysis in sol-gel reaction could result in high supersaturation, which leads to large number of small particles formed [59].

**Table 4.** Effect of calcination temperature on the properties of various Ag/Si composites.

| Composite          | Temp (°C)         | Time of Reaction (hr) | Size (nm)      | Shape                           | Crystallinity (Lattice Structure)  | Compositions                        | Ref. |
|--------------------|-------------------|-----------------------|----------------|---------------------------------|--|-------------------------------------|------|
| Ag/Si              | 200<br>350        | 4.0                   | 17.8           | -Semi-spherical<br>-Ellipsoidal | FCC<br>(200) – 44.6°   | Si-O-Si<br>Si-OH                    | [30] |
| Ag/Si              | 400<br>500<br>600 | 3.0                   | 7-11           | -Spherical<br>-Hollow tubes     | FCC<br>(111) – 38.1°<br>(200) – 44.3°<br>(220) – 64.5°<br>(311) – 77.5°                | Si-O-Si<br>Si-OH                    | [39] |
| Ag/Si              | 500<br>650        | 0.3                   | 23-26          | -Nanorod<br>-Quasi-spherical    | FCC<br>(111) – 38.51°<br>(200) – 44.41°<br>(220) – 64.61°<br>(311) – 81.61°            | Si-O-Si<br>Si-OH                    | [60] |
| Ag/Si              | 550               | 5                     | nd             | Hexagonal mesostructured        | (111)<br>(110)<br>(200)<br>Between 0.5° and 1.8°                                       | Si-O-M<br>Si-OH<br>H-O-H<br>Si-O-Ag | [61] |
| Polypyrrole /Ag/Si | 100               | 20                    | 20             | Honeycomb with hexagonal pores  | (111) – 38.23°<br>(200) – 44.47°<br>(220) – 64.48°<br>(311) – 77.31°<br>(222) – 81.73° | C, N, Ag, Si, O                     | [62] |
| Ag/Si              | 450<br>750        | 3                     | 32.97<br>25.18 | Spherical                       | (111) -38.1°<br>(200) - 44.3°<br>(220) – 64.4°   | Ag, Si, O                           | [50] |

From the collected data of the previous studies, the diffraction peaks for low and high calcined temperatures were assigned to planes (100), (200), (220), and (311), in accordance to the powder diffraction data files (JCPDS). The XRD analysis revealed that the composites were of face-centered cubic (FCC) and crystalline in nature. It was found that a higher calcination temperature results in an increased crystal size. Based on observations from Table 4, strong bands of Si-O-Si and Si-OH bonds stretching vibration were present in the composites as a result of calcination. However, at higher calcination temperatures, the Si-OH bands were no longer visible.

### 3.5. Physicochemical Properties of Ag/Si Composite

It is essential to characterize the synthesized Ag/Si composite to evaluate its physicochemical properties, such as surface charge, size, crystallinity, morphology, form, elemental composition, and surface chemistry. The physicochemical properties of various Ag/Si composites synthesized using different techniques are outlined in the following sub-section.

### 3.6. Shape and Size of Ag/Si Composite

Microscopy was extensively employed in evaluating the morphological properties of the synthesized Ag/Si composites.



Scanning electron microscopy (SEM) is an analytical technique used to evaluate the morphological aspects of micro- to nanoscale particles, including the shape, size, and distribution. In the characterization of Ag/Si composite, the surface of synthesized composite is scanned with a high-energy electron beam from SEM instrument to generate backscattered electrons that disclose the typical features and qualities of synthesized Ag/Si composite. Transmission electron microscopy (TEM), on the other hand provides the same function as SEM, but its greater resolution and magnification make it more effective for distinguishing between amorphous and crystalline structures using the chosen area electron diffraction approach. In addition, TEM outperforms SEM in measuring the average particle size of extremely small nanoparticles. According to the pie chart in Figure 2, the most reported diameter range of AgNPs decorated on Si substrate was of 1-20 nm (54.55%).

Smaller sized AgNPs of less than 100 nm diameter are expected to be more cytotoxic. When released into wastewater, they are quickly absorbed by aquatic life and could easily infiltrate the cell and localize into the nucleus if transmitted to a human cell. According to Figure 2, 4.55% of AgNPs decorated on Si substrate exhibited size of greater than 100 nm. Larger sized particles with diameters of more than 100 nm, on the other hand, demonstrate lower toxicity. However, it has been noted that an increased size of Ag/Si composite could limit its performance as a catalyst in environmental cleanup. As a result, fine-tuning the size of Ag/Si composites is critical in improving their capabilities, particularly as a catalyst for water treatment.

The shape of Ag/Si composite is a significant piece of information that determines its physical and chemical properties as a catalyst for pollutant removal. According to several prior studies, the catalytic activity of nanoparticles is

highly dependent on the NP-support contact area, i.e., the particles' shape [7,63,64]. Haruta's research group [65] observed that hemispherical particles performed better than spherical particles when different preparation techniques were utilized. Catalytic reactions may also occur at the perimeter interfaces of nanoparticles, where the proportion of step sites increases considerably with decreasing particle size, according to these findings.

TEM is an effective method for determining the shape of an Ag/Si composite. Even at low magnifications, TEM is capable to identify differences in contrast due to atomic weight and lattice direction. The method of preparation practiced is critical for synthesizing the various shapes of Ag/Si composites. According to Figure 3, the shapes of synthesized Ag/Si composites of mostly spherical (55.45%) or quasi-spherical (13.64%) were reported. AFM has been employed by several research groups to assess the surface roughness and topography of Ag/Si composites. Bois et. al. 2008 [66] revealed mesoporous structures of silica covered with 10 nm diameter AgNPs in AFM images of synthesized Ag/Si composite.

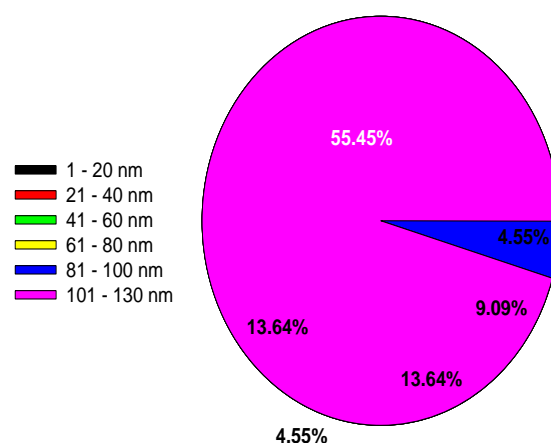


**Figure 2.** Size distribution of Ag/Si composites from literatures.

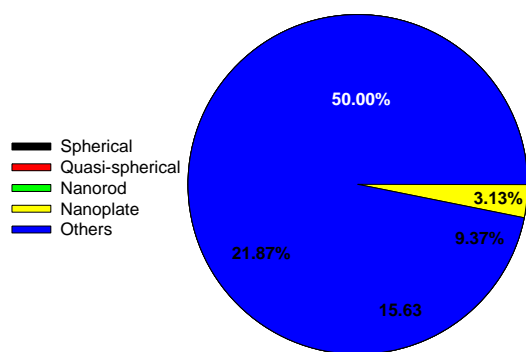


**Figure 3.** Shape of AgNPs decorated on Si substrate reported in literatures.

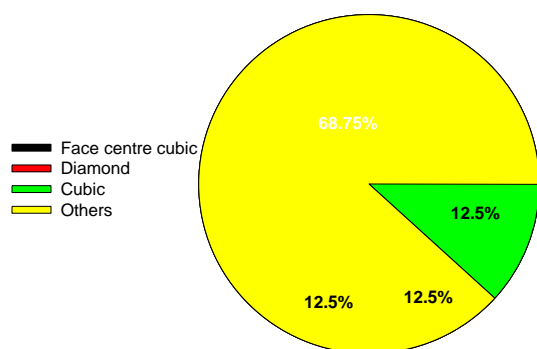


**Figure 4.** Crystallinity structure of various Ag/Si composites from literatures.

The elemental composition of a synthesized Ag/Si composite could be quantitatively determined using EDX. The collision of electrons with nanoparticles results in the generation of X-rays by an energy-dispersive X-ray. In [38] reported quasi-spherical AgNPs decoration on hydrated SiO<sub>2</sub> substrate. From EDX analysis, the intensity of the Si and O peaks was very high in comparison to that of Ag, implying few amounts of AgNPs decorated over hydrated SiO<sub>2</sub>. In addition, C and N peaks were observed possibly due to contribution from polydopamine (PDA) as adhesive.

XRD analysis is generally used for phase identification and characterization of the crystal structure of nanoparticles. In this analysis, X-rays penetrate into the nanomaterial and the resulting diffraction pattern is compared with standards to obtain structural information. Figure 4 discloses face-centered cubic as the major lattice structure of Ag/Si composites as reported

by previous studies (68.75%), followed by diamond crystal structure (12.50%), cubic crystalline, and other crystal lattices.

Peaks of XRD patterns corresponding to the planes (111), (200), (220), and (111) were identified by analyzing data from prior research (311). Moreover, the absence of peaks indicates the presence of amorphous SiO<sub>2</sub>.

A composite with a high concentration of metal precursor and a high intensity demonstrates efficient X-rays diffraction. Pure metal precursors, such as silver nitrate (AgNO<sub>3</sub>), exhibit crystalline peaks of crisp and strong features [67]. These peaks indicated that the samples were highly crystalline. It was observed that a high concentration metal precursor demonstrates a highly crystalline structure. The corresponding peaks of 2 indicate that the structure of the AgNPs was of face-centered cubic.

#### 4. CONCLUSION

This review paper aims to identify the physicochemical properties of Ag/Si composite using analyses of TEM, SEM, XRD, and EDX to determine the morphology, crystallinity, and chemical compositions of the sample. Three factors have been studied to synthesize the Ag/Si composite; concentration of metal precursor, temperature and time of reaction, and calcination temperature. The findings disclosed that increasing the concentration of metal precursor's results in bigger particle sizes. At higher concentrations of precursor, the agglomeration of particles may be associated with the higher surface energy. For the effect of retention time, a higher retention time could lead to the formation of larger diameter particles. However, at lower retention time, agglomeration of AgNPs in composite could occur which consequently produces smaller particles compared to using higher retention time. Therefore, the higher is the retention time, more AgNPs are immobilized onto the surface of SiNPs. For

the effect of reaction temperature, high temperatures favor nucleation while low temperatures promote particles growth, where the particle size would decrease as the temperature of reaction increases and vice versa. According to XRD analysis, higher intensity and narrower peaks were observed at higher reaction temperatures. Moreover, most of the samples indicate a crystalline structure based on the peaks observed at  $2\theta$  corresponding to the planes (111), (200), (220), and (311). The Ag/Si composites also demonstrated the compositions of Si and Ag. EDX analysis has been practiced in few studies to investigate the elements present in the Ag/Si composites. Ag, Si, C, N, and O components were observed in the composites based on EDX analysis. At higher calcination temperatures, it was found that the size of the particles was larger and exhibiting the development of AgNPs. However, agglomeration may occur for larger particles. In conclusion, the

uniqueness of Ag/Si composite from the novel synthesis strategy, as well as the choice and combination of Ag/Si composite at optimized concentration, retention time, temperature, and calcination temperature, may enhance its properties and performance as a catalyst for environmental remediation.

#### ACKNOWLEDGEMENT

This research was supported by the Malaysia Ministry of Higher Education – Fundamental Research Grant Scheme (FRGS/1/2021/STG05/UiTM/02/9). The authors also acknowledge the grants MIH-(008/2020) and 100-TNCPI/PRI 16/6/2 (029/2020), as well as Universiti Teknologi MARA, Cawangan Pulau Pinang for providing aid and assistance for this research.

#### CONFLICT OF INTEREST

The authors declare that they have no conflict of interest.

#### REFERENCES

1. Silva, G. A., "Introduction to nanotechnology and its applications to medicine", *Surg. Neurol.*, (2004) 61(3) 216-20. <https://doi.org/10.1016/j.surneu.2003.09.036>
2. Li, D., Liu, Y., Wu, N., "Application progress of nanotechnology in regenerative medicine of diabetes mellitus", *Diabetes Res. Clin. Pract.*, (2022) 109966. <https://doi.org/10.1016/j.diabres.2022.109966>
3. Majid, A., Faraj, H. R., "Green Synthesis of Copper Nanoparticles using Aqueous Extract of Yerba Mate (Ilex Paraguariensis St. Hill) and its Anticancer Activity", *Int. J. Nanosci. Nanotechnol.*, (2022) 18(2) 99-108.
4. Isa, N., Mohamad Nor, N., Wan Kamis, W. Z., Tan, W. K., Kawamura, G., Matsuda, A., "Anodized TiO<sub>2</sub> nanotubes using Ti wire in fluorinated ethylene glycol with air bubbles for removal of methylene blue dye", *J. Appl. Electrochem.*, (2022) 52(1) 173-88. <https://doi.org/10.1007/s10800-021-01644-z>
5. Rizvi, S. S. H., Moraru, C. I., Bouwmeester, H., Kampers, F. W. H., Cheng, Y., "Nanotechnology and food safety" *In: Ensuring global food safety*, (2022) 325-40.
6. Gattoo, M. A., Naseem, S., Arfat, M. Y., Mahmood Dar, A., Qasim, K., Zubair, S., "Physicochemical properties of nanomaterials: implication in associated toxic manifestations.", *Biomed Res. Int.*, (2014) 14. <https://doi.org/10.1155/2014/498420>
7. Isa, N., Wan Kamis, W. Z., Inderan, V., Husin, N. I., Ahmad, F. N., Bashir, N. H., "Shape, size and dispersion of plant-driven silver nanoparticles for removal of methylene blue dyes", *J. Phys. Conf. Ser.*, (2019) 13-49. <https://doi.org/10.1088/1742-6596/1349/1/012115>
8. Isa, N., Sarijo, S. H., Aziz, A., Lockman, Z. "Synthesis colloidal *Kyllinga brevifolia*-mediated silver nanoparticles at different temperature for methylene blue removal", *AIP Conf. Proc.*, (2017) 1877. <https://doi.org/10.1063/1.4999887>
9. Mohamad, N. N., Basir, M. R., Mahmood, A., Bakhari, N. A., Mydin, M. M., Arshad, N. M., "Synthesis of Silver Nanoparticles Using Beijing Grass Extract as Reducing Agent and The Comparative Study of AgNPs Toxicity", *Int. J. Electroact. Mater.*, (2022) (10) 1-11.
10. Isa, N., Bakhari, N. A., Sarijo, S. H., Aziz, A., Lockman, Z., "Kyllinga brevifolia mediated greener silver nanoparticles", *AIP Conference Proceedings*, (2017) 20012. <https://doi.org/10.1063/1.5010449>
11. Tiri, R.N.E., Gulbagca, F., Aygun, A., Cherif, A., Sen, F. "Biosynthesis of Ag-Pt bimetallic nanoparticles using propolis extract: Antibacterial effects and catalytic activity on NaBH<sub>4</sub> hydrolysis", *Environ. Res.*, 206 (2022) 112622. <https://doi.org/10.1016/j.envres.2021.112622>
12. Scala, A., Neri, G., Micale, N., Cordaro, M., Piperno, A. "State of the Art on Green Route Synthesis of

- Gold/Silver Bimetallic Nanoparticles”, *Molecules*, 27(3) (2022) 11-34.
13. Wei, R., Tang, N., Jiang, L., Yang, J., Guo, J., Yuan, X., “Bimetallic nanoparticles meet polymeric carbon nitride: Fabrications, catalytic applications and perspectives”, *Coord. Chem. Rev.*, 462 (2022) 214500. <https://doi.org/10.1016/j.ccr.2022.214500>
  14. Isa, N., Kian, T. W., Kawamura, G., Matsuda, A., Lockman, Z. “Synthesis of TiO<sub>2</sub> Nanotubes Decorated with Ag Nanoparticles (TNTs/AgNPs) For Visible Light Degradation of Methylene Blue”, *Journal of Physics: Conference Series*, (2018) 12105. <https://doi.org/10.1088/1742-6596/1082/1/012105>
  15. Alalwan, H. A., Alminshid, A. H., Mohammed, M. M., Hussein, S. A. M., Mohammed, M. F. “Employing Synthesized MgO-SiO<sub>2</sub> Nanoparticles as Catalysts in Ethanol Conversion to 1,3-Butadiene”, *Int. J. Nanosci. Nanotechnol.*, 18(3) (2022) 157-166.
  16. Basnet, S., Shah, S., Joshi, R., Pandit, R. “Investigation of Compressive Strength of Cement/Silica Nanocomposite Using Synthesized Silica Nanoparticles from Sugarcane Bagasse Ash .”, *Int. J. Nanosci. Nanotechnol.*, 18(2) (2022) 93-98.
  17. Chandra Sekhar, D., Diwakar, B. S., Madhavi, N., “Silica Coated Magnetic Nanoparticles forical Biolog Applications”, *Int. J. Nanosci. Nanotechnol.*, 16(4) (2020) 209-217.
  18. Lin, C., Liu, H., Guo, M., Zhao, Y., Su, X., Zhang, P., “Plasmon-induced broad spectrum photocatalytic overall water splitting: Through non-noble bimetal nanoparticles hybrid with reduced graphene oxide”, *Colloids Surfaces A Physicochem. Eng. Asp.*, 646 (2022) 128962. <https://doi.org/10.1016/j.colsurfa.2022.128962>
  19. Cuba-Supanta, G., Guerrero-Sanchez, J., Rojas-Tapia, J., Landauro, C. V, Rojas-Ayala, C., Takeuchi, N., “An atomistic study on the structural and thermodynamic properties of Al-Fe bimetallic nanoparticles during melting and solidification: The role of size and composition”, *Mater. Chem. Phys.*, 282 (2022) 125936. <https://doi.org/10.1016/j.matchemphys.2022.125936>
  20. Zhong, X., Yuan, P., Wei, Y., Liu, D., Losic, D., Li, M. “Coupling Natural Halloysite Nanotubes and Bimetallic Pt-Au Alloy Nanoparticles for Highly Efficient and Selective Oxidation of 5-Hydroxymethylfurfural to 2, 5-Furandicarboxylic Acid”, *ACS Appl. Mater. & Interfaces*, 14(3) (2022) 3949-3960. <https://doi.org/10.1021/acsami.1c18788>
  21. Pankaj, P., Bhattacharyya, S., Chatterjee, S. “Competition of core-shell and Janus morphology in bimetallic nanoparticles: Insights from a phase-field model”, *Acta Mater.*, 233 (2022) 117933. <https://doi.org/10.1016/j.actamat.2022.117933>
  22. Kuo, C. shun, Kuo, D. T. F., Chang, A., Wang, K., Chou, P. H., Shih, Y. hsin. “Rapid debromination of tetrabromobisphenol A by Cu/Fe bimetallic nanoparticles in water, its mechanisms, and genotoxicity after treatments”, *J. Hazard. Mater.*, 432 (2022) 128630. <https://doi.org/10.1016/j.jhazmat.2022.128630>
  23. Kang, H., Buchman, J. T., Rodriguez, R. S., Ring, H. L., He, J., Bantz, K. C., “Stabilization of silver and gold nanoparticles: preservation and improvement of plasmonic functionalities”, *Chem. Rev.*, 119(1) (2018) 664-699.
  24. Modekwe, H. U., Mamo, M., Moothi, K., Daramola, M. O. “Synthesis of bimetallic NiMo/MgO catalyst for catalytic conversion of waste plastics (polypropylene) to carbon nanotubes (CNTs) via chemical vapour deposition method”, *Mater. Today Proc.*, 38 (2021) 549-552. <https://doi.org/10.1016/j.matpr.2020.02.398>
  25. Yang, Y., Saoud, K. M., Abdelsayed, V., Glaspell, G., Deevi, S., El-Shall, M. S., “Vapor phase synthesis of supported Pd, Au, and unsupported bimetallic nanoparticle catalysts for CO oxidation”, *Catal. Commun.*, 7(5) (2006) 281-294. <https://doi.org/10.1016/j.catcom.2005.11.014>
  26. Isa, N., Lockman, Z. “Methylene blue dye removal on silver nanoparticles reduced by *Kyllinga brevifolia*”, *Environ. Sci. Pollut. Res.* (2019);26(11):11482 - 11495. <https://doi.org/10.1007/s11356-019-04583-7>
  27. Isa, N., Osman, M.S., Abdul Hamid, H., Inderan, V., Lockman, Z. “Studies of surface plasmon resonance of silver nanoparticles reduced by aqueous extract of shortleaf spikesedge and their catalytic activity”, *Int. J. Phytoremediation.*, (2022) <https://doi.org/10.1007/s11356-019-04583-7>
  28. Finn, R. C., Zubieta, J. “A New Class of Organic- Inorganic Hybrid Materials: Hydrothermal Synthesis and Structural Characterization of Bimetallic Organophosphonate Oxide Phases of the Mo/Cu/O/RPO<sub>32</sub>-Family”, *Inorg. Chem.*, 40(11) (2001) 2466 - 1277. <https://doi.org/10.1021/ic0100018>
  29. Mirzajani, R., Karimi, S. “Ultrasonic assisted synthesis of magnetic Ni-Ag bimetallic nanoparticles supported on reduced graphene oxide for sonochemical simultaneous removal of sunset yellow and tartrazine dyes by response surface optimization: Application of derivative spectrophot”, *Ultrason. Sonochem.*, 50 (2019) 239-250. <https://doi.org/10.1016/j.ultsonch.2018.09.022>
  30. Duhan, S., Kishore, N., Aghamkar, P., Devi, S., “Preparation and characterization of sol-gel derived silver-silica nanocomposite”, *J. Alloys Compd.*, 507(1) (2010) 101-114. <https://doi.org/10.1016/j.jallcom.2010.07.107>
  31. Khan, A., Shamsi, M. H., Choi, T. S. “Correlating dynamical mechanical properties with temperature and clay composition of polymer-clay nanocomposites”, *Comput. Mater. Sci.*, 45(2) (2009) 257-265. <https://doi.org/10.1016/j.commatsci.2008.09.027>

32. Chen, J., Yu, Y., Chen, J., Li, H., Ji, J., Liu, D., "Chemical modification of palygorskite with maleic anhydride modified polypropylene: mechanical properties, morphology, and crystal structure of palygorskite/polypropylene nanocomposites", *Appl. Clay Sci.*, 115 (2015) 230-237. <https://doi.org/10.1016/j.clay.2015.07.012>
33. Abou-El-Sherbini, K. S., Amer, M. H. A., Abdel-Aziz, M. S., Hamzawy, E. M. A., Sharmoukh, W., Elnagar, M. M., "Encapsulation of Biosynthesized Nanosilver in Silica Composites for Sustainable Antimicrobial Functionality", *Glob. Challenges*, 2(10) (2018) 1800048. <https://doi.org/10.1002/gch2.201800048>
34. Kobayashi, Y., Katakami, H., Mine, E., Nagao, D., Konno, M., "Silica coating of silver nanoparticles using a modified Stöber method" 283 (2005) 392 - 396. <https://doi.org/10.1016/j.jcis.2004.08.184>
35. Inglezakis, A., Korobeinyk, V. J., "Silver Nanoparticles Synthesised within the Silica Matrix in Hyperstoichiometrical of Mercury from Aqueous Solutions Silver Nanoparticles Synthesised within the Silica Matrix in Hyperstoichiometrical of Mercury from Aqueous Solutions", (2018) <https://doi.org/10.1088/1755-1315/182/1/012013>
36. Sembiring, S., Riyanto, A., Firdaus, I., Situmeang, R. "Structure and properties of silver-silica composite", 66(2) (2022) 167-177.
37. Joardar, S., Adams, M. L., Biswas, R., Deodhar, G. V., Metzger, K. E., Dewese, K., "Direct synthesis of silver nanoparticles modified spherical mesoporous silica as efficient antibacterial materials", *Microporous Mesoporous Mater.*, 313 (2021) 110824. <https://doi.org/10.1016/j.micromeso.2020.110824>
38. Das, T. K., Ganguly, S., Bhawal, P., Remanan, S., Ghosh, S., Das, N. C. "A facile green synthesis of silver nanoparticles decorated silica nanocomposites using mussel inspired polydopamine chemistry and assessment its catalytic activity", *J. Environ. Chem. Eng.*, 6(6) (2018) 6989-7001. <https://doi.org/10.1016/j.jece.2018.10.067>
39. Wang, J. X., Wen, L. X., Wang, Z. H., Chen, J. F., "Immobilization of silver on hollow silica nanospheres and nanotubes and their antibacterial effects", *Mater. Chem. Phys.*, 96(1) (2006) 90-97. <https://doi.org/10.1016/j.matchemphys.2005.06.045>
40. Jasiorski, M., Łuszczuk, K., Baszczuk, A. "Morphology and absorption properties control of silver nanoparticles deposited on two types of sol-gel spherical silica substrates", *J. Alloys Compd.*, 588 (2014) 70-74. <https://doi.org/10.1016/j.jallcom.2013.10.244>
41. Ahmad, T., Wani, I. A., Ahmed, J., Al-Hartomy, O. A. "Effect of gold ion concentration on size and properties of gold nanoparticles in TritonX-100 based inverse microemulsions", *Appl. Nanosci.*, 4(4) (2014) 491-498. <https://doi.org/10.1007/s13204-013-0224-y>
42. Sibiya, P. N., Moloto, M. J. "Effect of precursor concentration and pH on the shape and size of starch capped silver selenide (Ag<sub>2</sub>Se) nanoparticles", *Chalcogenide Lett.*, 11 (2014) 112-123.
43. Watanabe, T., Tochikubo, F., Hautanen, J., Kauppinen, E. I., "Review of particle agglomeration", *J. Aerosol Sci.*, 26 (1995) 2-6. [https://doi.org/10.1016/0021-8502\(95\)96917-V](https://doi.org/10.1016/0021-8502(95)96917-V)
44. Ashraf, M. A., Peng, W., Zare, Y., Rhee, K. Y. "Effects of size and aggregation/agglomeration of nanoparticles on the interfacial/interphase properties and tensile strength of polymer nanocomposites", *Nanoscale Res. Lett.*, 13(1) (2018) 1-7. <https://doi.org/10.1186/s11671-018-2624-0>
45. Fernando, I., Zhou, Y. "Impact of pH on the stability, dissolution and aggregation kinetics of silver nanoparticles", *Chemosphere.*, 216 (2019) 297-305. <https://doi.org/10.1016/j.chemosphere.2018.10.122>
46. Oves, M., Rauf, M.A., Aslam, M., Qari, H. A., Sonbol, H., Ahmad, I., "Green synthesis of silver nanoparticles by Conocarpus Lancifolius plant extract and their antimicrobial and anticancer activities", *Saudi J. Biol. Sci.*, 29(1) (2022) 460-471. <https://doi.org/10.1016/j.sjbs.2021.09.007>
47. Prasad, R. "Synthesis of Silver Nanoparticles in Photosynthetic Plants", (2014).
48. Mohamad, N. N., Mahmood, A., Bakhari, N. A., Mydin, M. M., Arshad, N. M., Isa, N., "Studies on Surface Plasmon Resonance of Murdannia loriformis Silver Nanoparticles", *Journal of Physics: Conference Series*. (2021) 120-124. <https://doi.org/10.1088/1742-6596/2129/1/012084>
49. Payami, R., Ghorbanpour, M., Parchehbaf Jadid, A. "Antibacterial silver-doped bioactive silica gel production using molten salt method", *J. Nanostructure Chem.*, 6(3) (2016) 215-221. <https://doi.org/10.1007/s40097-016-0193-2>
50. Devi, P., Deepak, S. "Synthesis , characterization and bactericidal activity of silica / silver core-shell nanoparticles", (2014). <https://doi.org/10.1007/s10856-014-5165-9>
51. Hagura, N., Widiyastuti, W., Iskandar, F., Okuyama, K. "Characterization of silica-coated silver nanoparticles prepared by a reverse micelle and hydrolysis - condensation process", *Chem. Eng. J.*, 156(1) (2010) 200-205. <https://doi.org/10.1016/j.cej.2009.10.024>
52. Lee, J. M., Kim, D. W., Kim, T. H., Oh, S. G., "Facile route for preparation of silica-silver heterogeneous nanocomposite particles using alcohol reduction method", *Mater. Lett.*, 61(7) (2007) 1558-1562. <https://doi.org/10.1016/j.matlet.2006.07.078>
53. Kumar, B., Smita, K., Cumbal, L., Debut, A., "Ionic liquid based silica tuned silver nanoparticles : Novel approach for fabrication", (2015) 31-74. <https://doi.org/10.1080/15533174.2015.1004451>

54. Purdy, S. C., Muscat, A. J. "Coating nonfunctionalized silica spheres with a high density of discrete silver nanoparticles", *J. Nanoparticle Res.*, 18(3) (2016) 1-10. <https://doi.org/10.1007/s11051-016-3371-8>
55. Li, W., Seal, S., Megan, E., Ramsdell, J., Scammon, K., Lelong, G., "Physical and optical properties of sol-gel nano-silver doped silica film on glass substrate as a function of heat-treatment temperature Physical and optical properties of sol-gel nano-silver doped silica film on glass substrate as a function of heat-treatment temperature", (2012). <https://doi.org/10.1063/1.1571215>
56. Mohamed, A. L., El-naggar, M. E., Shaheen, T. I., Hassabo, A. G. "Novel nano polymeric system containing biosynthesized core shell silver / silica nanoparticles for functionalization of cellulosic based material", *Microsyst. Technol.* (2015). <https://doi.org/10.1007/s00542-015-2776-0>
57. Patel, A.C., Li, S., Wang, C., Zhang, W., Wei, Y. "Electrospinning of Porous Silica Nanofibers Containing Silver Nanoparticles for Catalytic Applications", *Chem. Mater.*, 19(6) (2007) 1231-1238. <https://doi.org/10.1021/cm061331z>
58. Pandey, S., Ramontja, J. "Sodium alginate stabilized silver nanoparticles - silica nanohybrid and their antibacterial characteristics", *Int. J. Biol. Macromol.*, 93 (2016) 712-723. <https://doi.org/10.1016/j.ijbiomac.2016.09.033>
59. Cao, G., Wang, Y. "Fundamentals of homogeneous nucleation", *Nanostructures Nanomater. Synth. Prop. Appl.*, 3 (2004) 68-79.
60. Abdal-hay, A., Hamdy, A. S., Abdel-Jaber, G. T., Barakat, N. A. M., Ebnalwaled, A. A., Khalil, K. A., "A facile manufacturing of Ag/SiO<sub>2</sub> nanofibers and nanoparticles composites via a simple hydrothermal plasma method", *Ceram. Int.*, 41(9) (2015) 12447-12452. <https://doi.org/10.1016/j.ceramint.2015.06.082>
61. Kunchakara, S., Ratan, A., Dutt, M., Shah, J., Kotnala, R. K., Singh, V. "Impedimetric humidity sensing studies of Ag doped MCM-41 mesoporous silica coated on silver sputtered interdigitated electrodes", *J. Phys. Chem. Solids.*, 145 (2020) 109531. <https://doi.org/10.1016/j.jpcs.2020.109531>
62. Saad, A., Cabet, E., Lilienbaum, A., Hamadi, S., Abderrabba, M., Chehimi, M. M. "Polypyrrole/Ag/mesoporous silica nanocomposite particles: Design by photopolymerization in aqueous medium and antibacterial activity", *J. Taiwan Inst. Chem. Eng.*, 80 (2017) 1022-1030. <https://doi.org/10.1016/j.jtice.2017.09.024>
63. Jia, C. J., Schüth, F. "Colloidal metal nanoparticles as a component of designed catalyst", *Phys. Chem. Chem. Phys.*, 13(7) (2011) 2457-2487.
64. Azhar, A. S., Kamis, W. Z. W., Hamid, H. A., Kassim, N. F.A., Isa, N., "Removal of Tartrazine Dye Using *Kyllinga Brevifolia* Extract And Silver Nanoparticles As Catalysts.", *Journal of Physics: Conference Series.*, (2021) 120-133. <https://doi.org/10.1088/1742-6596/2129/1/012033>
65. Haruta, M. "Nanoparticulate Gold Catalysts for Low-Temperature CO Oxidation", *ChemInform.*, 35 (2004) 35-48.
66. Laurence, B., Chassagneux, F., Parola, S., Francois, B., Battie, Y., Destouches, N., "Silver nanoparticles in a mesostructured silica film" (2008).
67. Katta, V. K. M., Dubey, R. S., "Green synthesis of silver nanoparticles using *Tagetes erecta* plant and investigation of their structural, optical, chemical and morphological properties", *Mater. Today Proc.* 45 (2021) 794-809. <https://doi.org/10.1016/j.matpr.2020.02.809>.